nature medicine

Matrix IGF-1 maintains bone mass by activation of mTOR in mesenchymal stem cells

Lingling Xian[1,2], Xiangwei Wu[1,2], Lijuan Pang[1,2], Michael Lou[1], Clifford J Rosen[3], Tao Qiu[1], Janet Crane[1,4], Frank Frassica[1], Liming Zhang[1], Juan Pablo Rodriguez[5], Xiaofeng Jia[6], Shoshana Yakar[7], Shouhong Xuan[8], Argiris Efstratiadis[8], Mei Wan[1] & Xu Cao[1]

Insulin-like growth factor 1 (IGF-1), the most abundant growth factor in the bone matrix, maintains bone mass in adulthood. We now report that IGF-1 released from the bone matrix during bone remodeling stimulates osteoblastic differentiation of recruited mesenchymal stem cells (MSCs) by activation of mammalian target of rapamycin (mTOR), thus maintaining proper bone microarchitecture and mass. Mice with knockout of the IGF-1 receptor (*Igf1r*) in their pre-osteoblastic cells showed lower bone mass and mineral deposition rates than wild-type mice. Further, MSCs from *Igf1r*$^{flox/flox}$ mice with *Igf1r* deleted by a Cre adenovirus *in vitro*, although recruited to the bone surface after implantation, were unable to differentiate into osteoblasts. We also found that the concentrations of IGF-1 in the bone matrix and marrow of aged rats were lower than in those of young rats and directly correlated with the age-related decrease in bone mass. Likewise, in age-related osteoporosis in humans, we found that bone marrow IGF-1 concentrations were 40% lower in individuals with osteoporosis than in individuals without osteoporosis. Notably, injection of IGF-1 plus IGF binding protein 3 (IGFBP3), but not injection of IGF-1 alone, increased the concentration of IGF-1 in the bone matrix and stimulated new bone formation in aged rats. Together, these results provide mechanistic insight into how IGF-1 maintains adult bone mass, while also providing a further rationale for its therapeutic targeting to treat age-related osteoporosis.

Bone mass peaks in mid or late adolescence, plateaus for several years and then inexorably declines to a point, usually in older individuals, during which there is increased skeletal fragility and, often times, establishment of osteoporosis[1–4]. Acquisition of peak bone mass (PBM) is thought to reduce the subsequent risk of bone fracture, whereas impaired acquisition of PBM or loss of bone during adolescence is associated with greater fracture risk. IGF-1 is a key factor in the endocrine regulation of body composition and is integral not only to the acquisition of PBM but also to the maintenance of bone mineral density (BMD)[5–9]. In particular, IGF-1 and several of its binding proteins positively correlate with bone mass and can act as independent predictors for the risk of osteoporosis and incident fractures[10–13].

The maintenance of adult bone mass is accomplished by skeletal remodeling[3,14]. This remodeling is precisely coordinated by the activities of osteoblasts and osteoclasts[15,16]. We have previously shown that in response to osteoclastic bone resorption, active transforming growth factor β 1 (TGF-β1) is released from the bone surface and recruits MSCs to bone-resorptive sites, where they undergo differentiation into mature osteoblasts, thus coupling bone resorption with bone formation[17]. However, the osteogenic nature of the microenvironment at bone-resorptive sites is not well known. IGF-1 is the most abundant growth factor that is deposited in the bone matrix[12,18–20] and has been implicated in the coupling process through its actions on MSC differentiation *in vitro*[21]. In this study, we found that the concentrations of IGF-1 in bone marrow and matrix were lower in aged rats than in young rats and were closely associated with the change in bone volume in these rats, whereas blood serum concentrations of IGF-1 remained relatively steady during aging. We also found that IGF-1 released from the bone matrix during bone resorption generates an osteogenic microenvironment and induces the differentiation of recruited MSCs for new bone formation. Notably, IGF-1 activates mTOR through the phosphoinositide-3-kinase (PI3K)–thymoma viral proto-oncogene 1 (Akt) pathway to induce differentiation of MSCs into osteoblasts. Thus, we postulate that a primary function of IGF-1 in the bone matrix is to maintain bone mass and skeletal homeostasis during bone remodeling.

RESULTS

Knockout of *Igf1r* impairs bone formation in adult mice

To understand the role of IGF-1 in the maintenance of bone mass during bone remodeling, we first examined whether knockout of IGF-1 type 1 receptor (*Igf1r*) in the osteoprogenitor cells committed

[1]Department of Orthopaedic Surgery, Johns Hopkins University School of Medicine, Baltimore, Maryland, USA. [2]School of Medicine, Shihezi University, Shihezi, Xinjiang, China. [3]Center for Clinical & Translational Research, Maine Medical Center Research Institute, Scarborough, Maine, USA. [4]Department of Pediatrics, Johns Hopkins University School of Medicine, Baltimore, Maryland, USA. [5]Laboratorio de Biología Celular, Instituto de Nutrición y Tecnología de los Alimentos (INTA), The University of Chile, Santiago, Chile. [6]Department of Biomedical Engineering, Johns Hopkins University School of Medicine, Baltimore, Maryland, USA. [7]Division of Endocrinology, Diabetes and Bone Diseases, Mount Sinai School of Medicine, New York, New York, USA. [8]Department of Genetics and Development, Columbia University, New York, New York, USA. Correspondence should be addressed to X.C. (xcao11@jhmi.edu).

Received 7 March; accepted 18 April; published online 24 June 2012; doi:10.1038/nm.2793

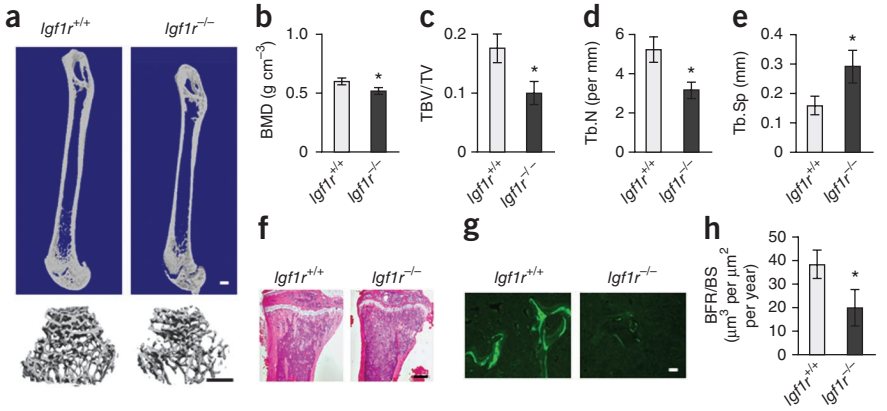

Figure 1 Low bone formation during bone remodeling in *Igf1r*$^{-/-}$ mice. (**a**) Representative micro-CT images of femora from a 3-month-old female *Igf1r*$^{-/-}$ mouse and a *Igf1r*$^{+/+}$ littermate. Scale bars, 1 mm. (**b**–**e**) Quantitative micro-CT analysis of the secondary spongiosa of proximal tibiae. Volumetric BMD (**b**), trabecular bone volume fraction (TBV/TV) (**c**), trabecular number (Tb.N) (**d**) and trabecular separation (Tb.Sp) (**e**) are shown. (**f**) H&E histological sections of tibiae from 3-month-old *Igf1r*$^{+/+}$ and *Igf1r*$^{-/-}$ mice. Scale bar, 1 mm. (**g**) Calcein double labeling of the metaphyseal trabecular bone at distal femora. Scale bar, 1 mm. (**h**) Bone formation rate per bone surface (BFR/BS). All data are mean ± s.e.m. $n = 10$. *$P < 0.05$ by one-way analysis of variance (ANOVA) followed by *t* test.

lower in 3-month-old *Igf1r*$^{-/-}$ mice than in their *Igf1r*$^{+/+}$ littermates of the same age (**Fig. 1a**,**b**). In particular, *Igf1r*$^{-/-}$ mice had a significantly lower trabecular bone volume and thickness and a greater trabecular bone space relative to their *Igf1r*$^{+/+}$ littermates ($P < 0.05$) (**Fig. 1c**–**e**).

We found similar results in H&E-stained sections and in histomorphometric analyses (**Fig. 1f** and **Supplementary Fig. 2**). The trabecular bone deficiency in female *Igf1r*$^{-/-}$ mice was more substantial than that in their male *Igf1r*$^{-/-}$ littermates (**Supplementary Fig. 2**), probably as a result of the dependency of IGF-1 action on estrogen in bone[23]. An analysis of calcein double labeling showed a lower dynamic bone formation rate in *Igf1r*$^{-/-}$ mice than in *Igf1r*$^{+/+}$ mice (**Fig. 1g**,**h**). Notably, periosteal bone formation was not affected in *Igf1r*$^{-/-}$ mice (**Supplementary Fig. 2g**). The results suggest a crucial role of IGF-1 in maintaining bone homeostasis in adult mice.

to the osteoblast lineage would reduce bone mass in adult mice. To achieve such a cell type-specific knockout, we crossed floxed *Igf1r* mice with Osx-GFP::Cre mice (which express a GFP-Cre fusion protein under the direction of the *Osx1* promoter[22]) to generate conditional *Igf1r* knockout mice (called here *Igf1r*$^{-/-}$) (**Supplementary Fig. 1a**,**b**) that express GFP in *Igf1r*-deficient cells. For both genders, the sizes of the newborn *Igf1r*$^{-/-}$ mice were similar to those of their *Osx1-GFP*::Cre; *Igf1r*$^{+/+}$ control littermates (here referred to as *Igf1r*$^{+/+}$) (**Supplementary Fig. 1c**–**f**). BMD was

Igf1r$^{-/-}$ mice have fewer mature osteoblasts than wild type

To determine if the reduced BMD in the *Igf1r*$^{-/-}$ mice was the result of reduced numbers of osteoblasts, we next measured their numbers at different stages of differentiation by immunostaining femur sections of *Igf1r*$^{-/-}$ mice and their *Igf1r*$^{+/+}$ littermates. The numbers of runt related transcription factor 2 (Runx2)$^+$ and osterix-positive osteoprogenitors on the bone surfaces of *Igf1r*$^{-/-}$ mice were not significantly ($P > 0.05$) different from those in their *Igf1r*$^{+/+}$ littermates (**Fig. 2a**–**c**); however, the number of osteocalcin-positive mature osteoblasts on

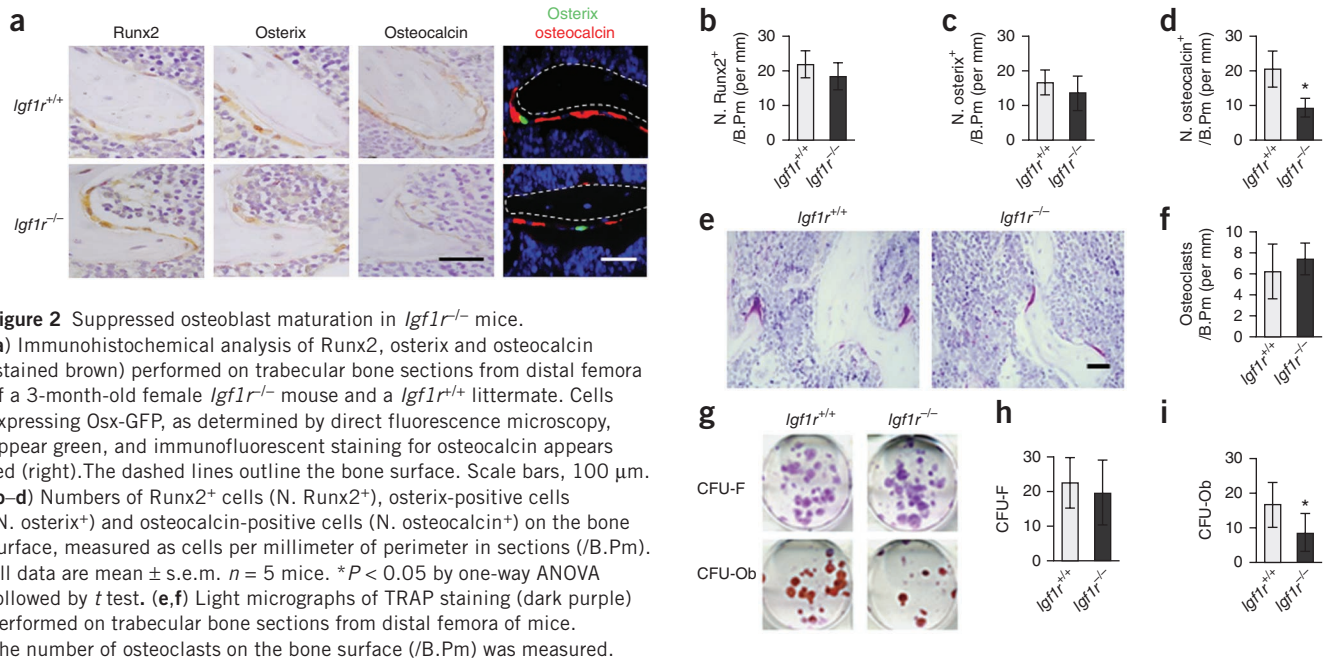

Figure 2 Suppressed osteoblast maturation in *Igf1r*$^{-/-}$ mice. (**a**) Immunohistochemical analysis of Runx2, osterix and osteocalcin (stained brown) performed on trabecular bone sections from distal femora of a 3-month-old female *Igf1r*$^{-/-}$ mouse and a *Igf1r*$^{+/+}$ littermate. Cells expressing Osx-GFP, as determined by direct fluorescence microscopy, appear green, and immunofluorescent staining for osteocalcin appears red (right).The dashed lines outline the bone surface. Scale bars, 100 μm. (**b**–**d**) Numbers of Runx2$^+$ cells (N. Runx2$^+$), osterix-positive cells (N. osterix$^+$) and osteocalcin-positive cells (N. osteocalcin$^+$) on the bone surface, measured as cells per millimeter of perimeter in sections (/B.Pm). All data are mean ± s.e.m. $n = 5$ mice. *$P < 0.05$ by one-way ANOVA followed by *t* test. (**e**,**f**) Light micrographs of TRAP staining (dark purple) performed on trabecular bone sections from distal femora of mice. The number of osteoclasts on the bone surface (/B.Pm) was measured. All data are mean ± s.e.m. $n = 10$ mice. *$P < 0.05$ by one-way ANOVA followed by *t* test. Scale bar, 100 μm. (**g**) CFU-F and CFU-Ob assays from harvested bone marrow of the mice, as indicated. Representative images of CFU-Fs stained with crystal violet (top) and representative images of CFU-Obs stained with Alizarin red (bottom). (**h**,**i**) Quantifications of the CFU-F and CFU-Ob assays. All data are the mean ± s.e.m. of triplicate cultures of bone marrow nucleated cells pooled from five individual mice. *$P < 0.05$ by one-way ANOVA followed by *t* test.

the bone surfaces of *Igf1r*$^{-/-}$ mice was significantly lower than in their *Igf1r*$^{+/+}$ littermates ($P < 0.05$) (**Fig. 2a**,**d**).

Additionally, as the *Igf1r*$^{-/-}$ mice also express GFP, this allowed us to visualize endogenous cells with specific deletion of *Igf1r* in the pre-osteoblasts *in vivo*. The *Igf1r*-deficient osteoprogenitors were therefore GFP^{+} and were located primarily at the bone surface. However, *Igf1r*$^{-/-}$ mice had fewer osteocalcin-positive mature osteoblasts than *Igf1r*$^{+/+}$ mice (**Fig. 2a**). The number of tartrate-resistant acid phosphatase (TRAP)$^{+}$ mature osteoclasts in *Igf1r*$^{-/-}$ mice was not significantly different than that in their *Igf1r*$^{+/+}$ littermates ($P > 0.05$) (**Fig. 2e**,**f**). Colony-forming unit fibroblast (CFU-F) and colony-forming unit osteoblast (CFU-Ob) assays showed that the number of CFU-Fs in the *Igf1r*$^{-/-}$ mice was not significantly different than the number in their *Igf1r*$^{+/+}$ littermates ($P > 0.05$) (**Fig. 2g**,**h**); however, the number of CFU-Obs was lower in the *Igf1r*$^{-/-}$ mice than in their *Igf1r*$^{+/+}$ littermates ($P < 0.05$) (**Fig. 2g–i**). This finding further indicates that the lower number of mature osteoblasts on the bone surfaces of *Igf1r*$^{-/-}$ mice was probably the result of reduced differentiation of MSCs recruited to bone remodeling sites.

IGF-1 induces osteoblast differentiation through mTOR

We then sought to elucidate the signaling mechanism of IGF-1–induced osteogenic differentiation of MSCs by isolating mouse bone marrow cells and sorting them by flow cytometry. We defined MSCs as positive for stem cell antigen (Sca-1) and intergin β-1 (CD29) and negative for CD45 and CD11b, which represents the hematopoietic lineage, as previously reported[17]. Treatment with the PI3K inhibitor, LY294002 (10 μM), or the mTOR inhibitor, rapamycin (20 nM), impaired the MSC-mediated mineralization that was induced by IGF-1 but did not affect their cell growth or survival (**Fig. 3a**). In addition, IGF-1 stimulated the phosphorylation of the IGF-1 receptor (IGF1R), insulin receptor substrate 1 (IRS1), PI3K, Akt and mTOR in MSCs. Although treatment of the MSCs with LY294002 reduced the phosphorylation of PI3K, Akt and mTOR, treatment with rapamycin inhibited only the phosphorylation of mTOR (**Fig. 3b**), indicating that IGF-1 activates mTOR through the PI3K-Akt pathway in MSCs.

We also knocked down *Irs1* in MSCs with *Irs1*-targeting siRNA, which resulted in an inhibition in the IGF-1–induced (20 ng ml^{-1}, 15 min) phosphorylation of PI3K, Akt and mTOR (**Fig. 3c**), confirming that IRS1 mediates the IGF-1–induced activation of mTOR. Notably, rapamycin inhibited the IGF-1–induced expression of markers of osteoblast differentiation such as osterix (*Sp7*), *Runx2*, alkaline phosphatase (*Alp*), osteocalcin (*Bglap*), osteoglycin (*Ogn*) and osteoactivin (*Gpnmb*) (**Supplementary Fig. 3**).

To investigate the role of mTOR in IGF-1–induced MSC differentiation *in vivo*, we isolated MSCs from *Igf1r*$^{flox/flox}$ mice and deleted *Igf1r* in them using an adenovirus expressing Cre with GFP (Ad-Cre-GFP) or an adenovirus expressing GFP only (Ad-GFP) as a control. We transplanted Ad-Cre-GFP–treated MSCs (Ad-Cre-GFP MSCs) or Ad-GFP–treated MSCs (Ad-GFP MSCs) embedded in Matrigel underneath the renal capsules of immune-deficient *Rag2*$^{-/-}$ mice and injected each group of mice with rapamycin (3 mg per kg of body weight) or vehicle daily for 4 weeks. Ad-GFP MSCs underwent osteoblast differentiation and mineralization underneath the renal capsule, as shown by H&E staining, Alizarin red staining and immunohistology of osteocalcin staining (**Fig. 3d**). Similar to the results of the Ad-Cre-GFP MSCs, treatment with rapamycin inhibited the osteoblast differentiation and mineralization of Ad-GFP MSCs (**Fig. 3d**). Furthermore, we subcutaneously injected 6-week-old wild-type

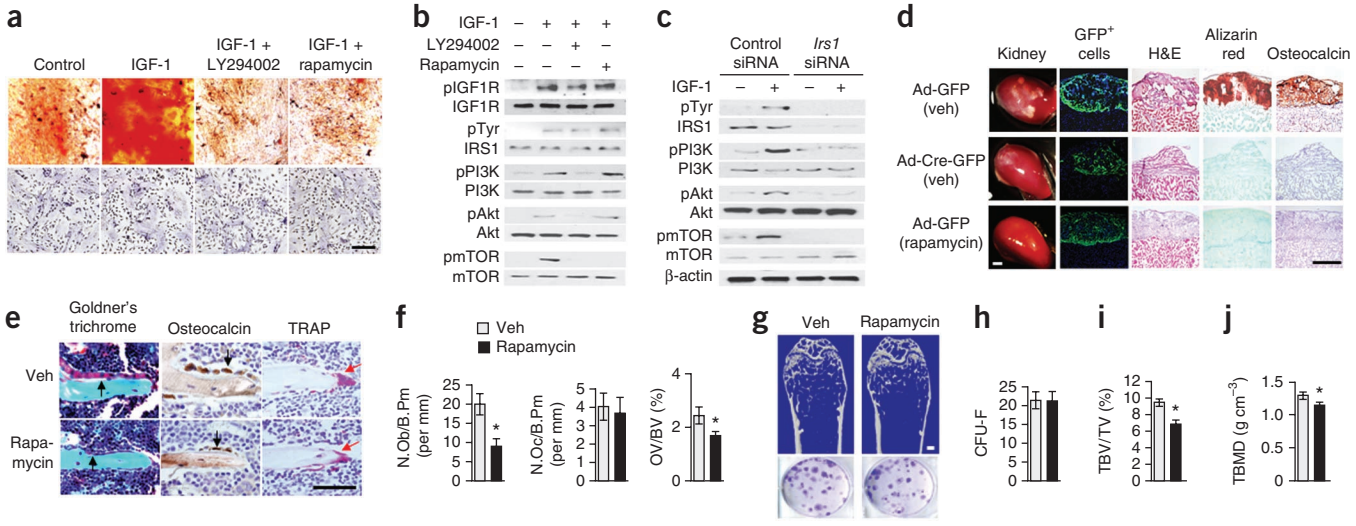

Figure 3 IGF-1 induces the osteoblastic differentiation of MSCs through the IRS-PI3K-Akt-mTOR pathway. (**a**) Alizarin red staining showing the osteoblastic differentiation of MSCs induced by IGF-1, as indicated (top). The number of live cells was determined by hematoxylin staining (bottom). Scale bar, 100 μm. (**b**) Western blot analysis of the IGF-1–induced phosphorylation of IGF1R (pIGF1R), phosphorylation of IRS1 at the tyrosine residue (pTyr), PI3K (pPI3K), Akt (pAkt) and mTOR (pmTOR) in MSCs treated with IGF-1 (20 ng ml^{-1}) or vehicle in the presence or absence of LY294002 (10 μM) or rapamycin (20 nM) for 15 min, as indicated. (**c**) Western blot analysis of the IGF-1–induced phosphorylation of IRS1, PI3K, Akt and mTOR in MSCs treated with IGF-1 after being transfected with *Irs1* siRNA or control siRNA. (**d**) IGF-1 induced the differentiation of MSCs underneath renal capsules. The renal sections were analyzed by direct GFP fluorescence visualization, H&E staining, Alizarin red staining or immunohistology for osteocalcin. Scale bars, 100 μm. Veh, vehicle. (**e**–**g**) Rapamycin impairs trabecular bone formation. (**e**) Representative images of mouse distal femora sections with Goldner's trichrome staining or staining for osteocalcin or TRAP. The black arrows indicate osteoblasts, and red arrows indicate osteoclasts. Scale bar, 100 μm. (**f**,**g**) Histomorphometric analysis of remodeling trabecular bone after treatment with rapamycin; shown are the number of osteoblasts (N.Ob) per bone perimeter, the number of osteoclasts (N.Oc) per bone perimeter, osteoid volume per bone volume (OV/BV; **f**) and representative micro-CT images of distal femora (**g**, top). Scale bar, 1 mm. (**g**–**j**) CFU-F assays (**g**(bottom),**h**), trabecular bone volume fraction (TBV/TV) (**i**) and the trabecular bone mineral density (TBMD) (**j**) are shown. All data are mean ± s.e.m. $n = 8$ mice. $^{*}P < 0.05$ by one-way ANOVA followed by *t* test.

C57BL/6 mice with rapamycin daily (3 mg per kg body weight per day) for 4 weeks. The numbers of osteocalcin-positive osteoblasts on the bone surfaces of the C57BL/6 rapamycin-injected mice were significantly lower than in vehicle-injected littermates ($P < 0.05$), whereas the number of osteoclasts was the same in the two groups (**Fig. 3e**,**f**). In the rapamycin-injected group of C57BL/6 mice, we observed significantly less new bone formation and a lower trabecular bone mass compared to the vehicle-injected group by trichrome staining and a micro computed tomography (micro-CT) analysis. However, the number of CFU-Fs was not affected by introduction of rapamycin in either group (**Fig. 3e**,**g**–**j** and **Supplementary Table 1**). In summary, IGF-1 activates mTOR through the IRS1-PI3K-Akt pathway to regulate the osteoblast differentiation of MSCs for bone formation.

IGF-1 from bone matrix induces differentiation of MSCs

We know that recruited MSCs at bone-resorptive sites undergo differentiation and contribute to new bone formation, but the osteogenic nature of the microenvironment at bone-resorptive sites is not well known. We therefore examined the amount of phosphorylated IGF1R in the bone-resorption areas by co-staining for IGF1R and TRAP$^+$ osteoclasts in mouse femora. We found phosphorylated IGF1R primarily at the bone surfaces along bone-resorptive sites, as defined by the presence of mature TRAP$^+$ osteoclasts, whereas we found the IGF1R$^+$ cells to be evenly distributed in the bone marrow (**Fig. 4a**). This suggests that active IGF-1 is released during osteoclastic bone resorption. After bone marrow transplantation of Ad-Cre-GFP or Ad-GFP MSCs, we identified bone-marrow–transplanted GFP-labeled mouse MSCs on the bone surfaces by immunostaining with an antibody to GFP and quantified these cells. We found no significant difference in the number of GFP$^+$ cells on the bone surfaces of the group transplanted with Ad-Cre-GFP MSCs and the group transplanted with Ad-GFP MSCs at 2 weeks after bone marrow transplantation (**Fig. 4b**,**c**). There were significantly more GFP$^+$ MSCs embedded in the bone matrix of mice transplanted with Ad-GFP MSCs than in the bone matrix of the mice transplanted with Ad-Cre-GFP MSCs at 4 weeks after transplantation (**Fig. 4b**,**d**). We analyzed the survival rate of the transplanted GFP-labeled MSCs in the bone marrow of these mice by flow cytometry 2 weeks after transplantation, and the results indicate that deletion of *Igf1r* did not affect the survival rate of the MSCs in the bone marrow (**Supplementary Fig. 4**).

We reasoned that the IGF-1 released from the bone matrix comprises the osteogenic microenvironment for the induction of osteoblast differentiation. We cultured osteoclast precursors or mature osteoclasts from wild-type C57BL/6 mice with or without bone slices *in vitro* and collected the culture media to examine the effects on the osteoblastic differentiation of MSCs. Bone-resorption–conditioned media (BRCM) from mature osteoclasts containing bone slices had the highest capability to induce alkaline phosphatase (ALP) activity, a marker for osteoblast differentiation (**Fig. 4e**). We detected IGF-1 only in the BRCM from mature osteoclasts plus bone slices but not in any other conditioned media (**Fig. 4f**). We found that BRCM stimulated the phosphorylation of IGF1R, IRS1, PI3K, Akt and mTOR within 1 h after treatment (**Fig. 4g**). Furthermore, addition of an antibody specific for IGF-1 to the BRCM significantly inhibited the activity of ALP ($P < 0.05$), whereas treating the mature osteoclasts plus bone slices BRCM with noggin (an antagonist for bone morphogenetic protein) and other antibodies against IGF-II and PGDF had no effect or a minimal effect on ALP activity (**Fig. 4h**), suggesting that IGF-1 is the primary factor for the osteogenic microenvironment at bone-resorptive sites. Deletion of *Igf1r* in MSCs isolated from *Igf1r*$^{flox/flox}$ mice blocked the osteoblast differentiation induced by BRCM, as evident by both ALP staining and Alizarin red staining (**Fig. 4i**,**j**). Thus, IGF-1 released from the bone matrix induces the osteoblast differentiation of MSCs recruited by TGF-β1 in the process of coupling bone resorption with bone formation.

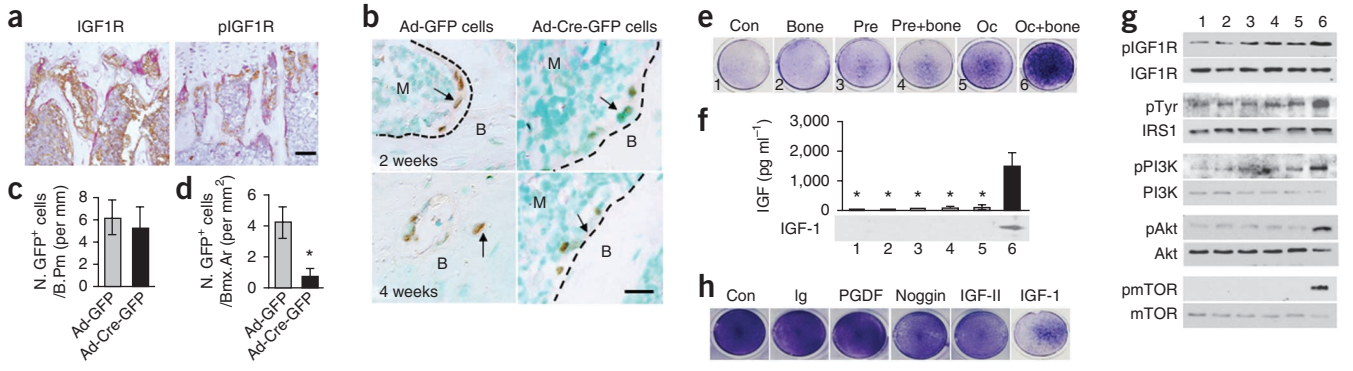

Figure 4 BRCM induces the osteogenic differentiation of MSCs. (**a**) Immunohistochemical analysis of the trabecular bone sections of mouse distal femora with antibodies to IGF1R (left) and pIGF1R (right). Scale bar, 200 μm. (**b**) Immunohistochemical analysis of femora sections of 3-month-old *Rag2*$^{-/-}$ mice transplanted with GFP-labeled mouse MSCs (Ad-GFP cells or Ad-Cre-GFP cells) by antibody to GFP. Scale bar, 100 μm. B, bone; M, bone marrow. The arrows point to GFP$^+$ cells (stained brown), and the dashed lines indicate the bone surface. (**c**,**d**) Quantification of GFP$^+$ cells on the bone surface 2 weeks after transplantation (N. GFP$^+$/B.Pm) or in the bone matrix 4 weeks after transplantation (N. GFP$^+$/Bmx.Ar). $n = 5$ mice. $^*P < 0.05$ by one-way ANOVA followed by *t* test. (**e**) ALP staining for the differentiation potentials of MSCs cultured in various conditioned media, as indicated. Con, medium only (1); bone, bone slice only (2); pre, osteoclast precursor culture (3); pre+bone, osteoclast precursors cultured with bone slice (4); oc, osteoclast culture (5); oc+bone, osteoclasts cultured with bone (6). (**f**) ELISA analysis of IGF-1 concentrations in the BRCM. $n = 3$ repeats of each BRCM. $^*P < 0.05$ by one-way ANOVA followed by Dunnett's test compared to the oc+bone group. All data are mean ± s.e.m. (**g**) Western blot analysis of the effects of various conditioned media on the phosphorylation of IGF1R, IRS1, PI3K, Akt and mTOR in MSCs. (**h**) ALP staining for the differentiation potentials of MSCs cultured in BRCM with the addition of individual neutralizing antibodies (to Ig, PGDF, IGF-II or IGF-1) or noggin, as indicated. Con, conditioned media with no antibody. (**i**,**j**) ALP staining (**i**) and Alizarin red staining (**j**) for the effect of BRCM on the differentiation potentials of MSCs isolated from *Igf1r*$^{flox/flox}$ mice by infection with Ad-Cre-GFP or Ad-GFP (**j**, top). Western blot analysis of IGF1R in MSCs (**j**, bottom).

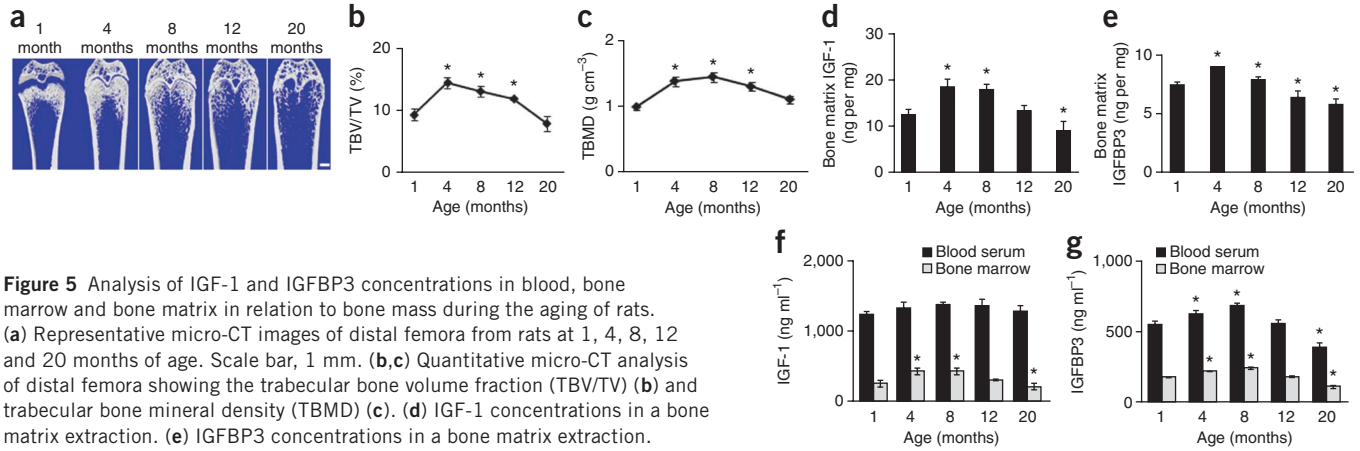

Figure 5 Analysis of IGF-1 and IGFBP3 concentrations in blood, bone marrow and bone matrix in relation to bone mass during the aging of rats. (**a**) Representative micro-CT images of distal femora from rats at 1, 4, 8, 12 and 20 months of age. Scale bar, 1 mm. (**b**,**c**) Quantitative micro-CT analysis of distal femora showing the trabecular bone volume fraction (TBV/TV) (**b**) and trabecular bone mineral density (TBMD) (**c**). (**d**) IGF-1 concentrations in a bone matrix extraction. (**e**) IGFBP3 concentrations in a bone matrix extraction. (**f**,**g**) Concentrations of IGF-1 (**f**) and IGFBP3 (**g**) in bone marrow and peripheral blood serum in rats at different ages. All data are the mean ± s.e.m. of triplicate repeats for each sample and ten individual rats for each time point. *$P < 0.05$ by one-way ANOVA followed by Dunnett's test compared to the group aged 1 month.

Age-related bone loss is associated with bone matrix IGF-1

We assessed the concentrations of IGF-1 and IGFBP3 in the bone matrix and its potential correlation with the bone mass of wild-type rats at ages 1, 4, 8, 12 and 20 months. We found that the bone volume and bone mass in these rats increased steadily from 1 to 8 months after birth and then decreased continuously from 8 months of age onwards (**Fig. 5a–c**). We also observed PBM at 8 months of age. Notably, changes in the concentrations of IGF-1 and IGFBP3 in the bone matrix of the rats were well correlated with the changes in bone mass described above (**Fig. 5d**,**e**), and the number of osteoblasts decreased with higher age (**Supplementary Fig. 5a**,**b**). In contrast, the concentration of IGF-1 in the blood serum was much higher than that in bone marrow at all ages and did not decrease considerably with age ascension (**Fig. 5f**). However, blood sera IGFBP3 concentrations decreased in an age-dependent manner (**Fig. 5g**). Of note, in humans, IGF-1 and IGFBP3 concentrations in the bone martrix were also correlated with the changes in bone mass over aging[12]. Notably, we found that in individuals with osteoporosis with hip fractures, the concentration of IGF-1 in their bone marrow was 40% lower than in controls with normal bone mass (**Supplementary Fig. 5d** and **Supplementary Table 2**).

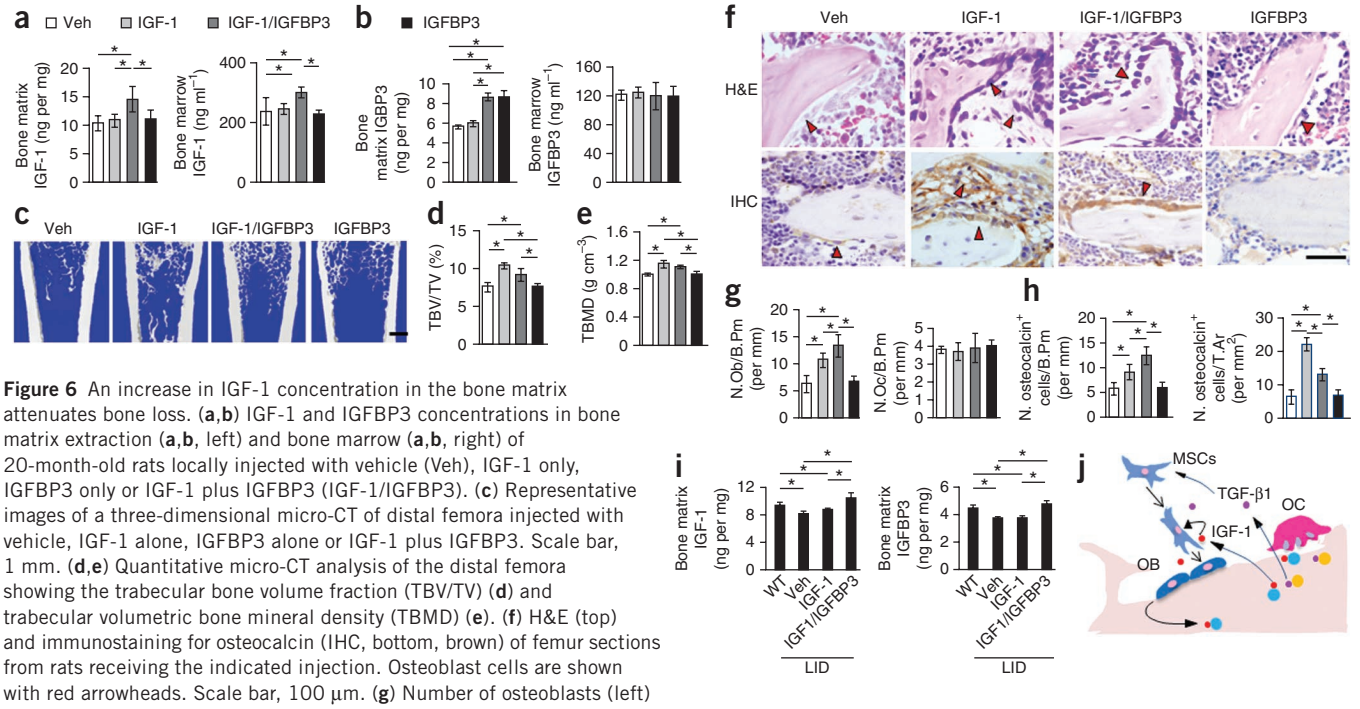

Figure 6 An increase in IGF-1 concentration in the bone matrix attenuates bone loss. (**a**,**b**) IGF-1 and IGFBP3 concentrations in bone matrix extraction (**a**,**b**, left) and bone marrow (**a**,**b**, right) of 20-month-old rats locally injected with vehicle (Veh), IGF-1 only, IGFBP3 only or IGF-1 plus IGFBP3 (IGF-1/IGFBP3). (**c**) Representative images of a three-dimensional micro-CT of distal femora injected with vehicle, IGF-1 alone, IGFBP3 alone or IGF-1 plus IGFBP3. Scale bar, 1 mm. (**d**,**e**) Quantitative micro-CT analysis of the distal femora showing the trabecular bone volume fraction (TBV/TV) (**d**) and trabecular volumetric bone mineral density (TBMD) (**e**). (**f**) H&E (top) and immunostaining for osteocalcin (IHC, bottom, brown) of femur sections from rats receiving the indicated injection. Osteoblast cells are shown with red arrowheads. Scale bar, 100 μm. (**g**) Number of osteoblasts (left) and osteoclasts (right) of remodeling trabecular bone quantified by histomorphometric analysis. (**h**) Quantification of osteocalcin-positive cells on the bone surface (left) and in the total tissue area (T.Ar, right). (**i**) Concentrations of IGF-1 (left) and IGFBP3 (right) in bone matrix extractions from LID mice or their wild-type littermates infused with vehicle, IGF-1 only or IGF-1 plus IGFBP3 by osmotic pumps. All data are mean ± s.e.m. $n = 10$ rats or mice. *$P < 0.05$ by one-way ANOVA followed by Bonferroni test. (**j**) Schematic diagram of bone matrix IGF-1–induced osteoblast differentiation of MSCs during bone remodeling. TGF-β1 recruits MSCs to the bone-resorptive site in response to osteoclastic bone resorption, and IGF-1 released from the bone matrix comprises the osteogenic microenvironment for the differentiation of recruited MSCs. OB, osteoblast; OC, osteoclast.

To determine whether aging affects the potency of IGF1R activation on MSCs, we isolated bone marrow cells from rats at 1, 4 and 20 months of age for CFU-F assays. We picked a single colony and then expanded, cultured and treated it with IGF-1 (20 ng ml^{-1}) for 10 min. We found no remarkable differences in IGF1R activation in MSCs from young (1 month of age), adult (4 months of age) or old (20 months of age) rats by western blot analysis (**Supplementary Fig. 5e**). The correlation of bone matrix IGF-1 concentrations with bone mass quantifications suggests a crucial role for bone matrix IGF-1 in the maintenance of bone mass.

Administration of IGF-1 plus IGFBP3 attenuates bone loss

To assess whether IGFBP3 binds IGF-1 in the extracellular matrix and enhances its activity, we injected vehicle, IGF-1, IGFBP3 or IGF-1 plus IGFBP3 into the distal femur cavity of 20-month-old rats once a week for 4 weeks. We measured the concentrations of IGF-1 and IGFBP3 in the serum, bone marrow and bone matrix 10 d after the last injection. The concentrations of IGF-1 in the bone matrix and marrow were significantly higher in rats injected with IGF-1 plus IGFBP3 than in rats injected with IGF-1 only, IGFBP3 only or vehicle ($P < 0.05$) (**Fig. 6a**). The concentrations of IGFBP3 in the bone matrix were also higher in the rats injected with IGF-1 plus IGFBP3 and IGFBP3 only relative to the vehicle and IGF-1 only groups (**Fig. 6b**). Blood serum IGF-1 and IGFBP3 concentrations were the same in all injection groups (**Supplementary Fig. 5f**). This suggests that IGFBP3 could regulate IGF-1 deposition in the bone matrix and its lifespan in the bone marrow.

Of note, both bone volume and bone density were higher in rats injected with IGF-1 only or IGF-1 plus IGFBP3 than those injected with IGFBP3 only or vehicle (**Fig. 6c–e**). However, bone formation in the rats injected with IGF-1 only occurred in clusters that were structurally deficient of natural trabecular bone, whereas rats injected with IGF-1 plus IGFBP3 had improvements in bone mass and in bone microarchitecture (**Fig. 6c–f**). An analysis of contralateral control samples indicated that such changes in the trabecular bone are limited only to the injected femur (**Supplementary Fig. 5g–i**). H&E staining and immunohistology for osteocalcin in femur sections showed that a large number of osteoblast-like cells or osteocalcin-positive osteoblasts were scattered throughout the bone marrow in the rats injected with IGF-1 only (**Fig. 6c**). Notably, in the rats injected with IGF-1 plus IGFBP3, we found osteocalcin-positive osteoblasts primarily on the bone surface (**Fig. 6g,h**). We also found that osteoclast numbers did not change significantly between any of the injection groups.

These results indicate that IGFBP3 mediates the association of IGF-1 to the bone extracellular matrix for *de novo* bone formation at the bone surface. We therefore examined whether circulating IGF-1 and IGFBP3 can target and become immobilized in the bone matrix. We infused IGF-1, IGF-1 plus IGFBP3 or vehicle into the circulations of 4-week-old mice with liver-specific deletion of the IGF-1 gene (LID mice) using osmotic pumps for 4 weeks. Infusion of IGF-1 plus IGFBP3 led to significantly higher concentrations ($P < 0.05$) of both IGF-1 and IGFBP3 in the bone matrix of LID mice (**Fig. 6i**), as well as enhanced trabecular bone formation ($P < 0.05$), relative to LID mice infused with IGF-1 alone or with vehicle (**Supplementary Table 3**). Our results suggest that IGFBPs such as IGFBP3 facilitate the deposition of IGF-1 in the bone matrix for its function during bone remodeling.

DISCUSSION

Bone formation is an energy-consuming metabolic process in which there are major events of bone matrix synthesis and mineralization by osteoblasts. IGF-1 regulates new bone formation by acting more as a differentiation factor than as a mitogen for osteoblastic cells. We found that IGF-1 induced the osteoblast differentiation of MSCs through activation of the mTOR signaling pathway. Inhibition of mTOR activity with rapamycin blocked the IGF-1–induced osteoblast differentiation of MSCs, as well as their mineralization.

mTOR is crucial as a signaling molecule contributing to both the whole organ and to cellular energy metabolism in response to nutrient availability and environmental stimuli[24]. The mTOR pathway, when genetically downregulated, increases life span and stem cell homeostasis in evolutionarily diverse organisms such as mammals[24]. IGF-1 is also a key determinant of body size and lifespan in animals. Our results indicate that the regulation of osteoblast differentiation from MSCs in the bone remodeling unit by IGF-1 through mTOR may help explain the mechanism behind the regulation of body size and longevity by IGF-1(refs. 25,26). In addition, the mTOR complex has emerged as a key regulator of cell migration and chemotaxis[27], suggesting that IGF-1 may also facilitate the recruitment of MSCs in the coupling process during bone remodeling. In the coupling process, active IGF-1, released from the bone matrix during the resorptive phase, induces differentiation of MSCs that were recruited by TGF-β1, which was also released during the resorptive phase (**Fig. 6j**).

Although most efforts to prevent fracture in osteoporosis have been directed at inhibiting age-related bone loss, growing evidence suggests that bone mass maintenance during early adult life is a key contributor to bone strength during aging[12,28–31]. IGF-1 is the most abundant growth factor that is deposited in the bone matrix throughout the mammalian lifetime[32]. IGF-1 concentrations in the circulation and the bone matrix decline substantially with age in both men and women[33–35], probably as a result of a reduction in growth hormone secretion. Notably, a previous study reported that skeletal IGF-1 content in human bones also declines almost 60% between the ages of 20 and 60 years[36]. Circulating IGF-1 concentrations are much higher in rodents than in humans, and the circulating concentrations of IGF-II in humans are higher than those of IGF-1. Furthermore, IGF-1 concentrations in blood serum do not change with age in rats, whereas in humans they progressively decline with age to less than 100 ng ml^{-1} at around 60 years of age. However, despite these differences, it should be noted that the concentrations of IGF-1 in the bone matrix in both humans and rodents decrease with age.

In this study, we found that IGF-1 concentrations were significantly ($P < 0.05$) lower in the bone marrow of individuals with osteoporosis with low bone mass compared to individuals with osteoarthritis with normal bone mass. Although the subjects with osteoarthritis and those with osteoporosis were age matched, one limitation of our study was that we could not evaluate healthy aged controls. Despite this limitation and consistent with our findings, a previous clinical trial reported that individuals with a hip fracture that were treated with a complex of IGF-1 plus IGFBP3 had marked functional improvements and a blunting in femoral bone loss compared to vehicle-treated control subjects with osteoporosis after hip fracture[37]. Administration of IGF-1 alone has not been shown to enhance bone mass or improve functional outcomes in older individuals. Currently available clinical observations and our rodent results suggest that the essential pool of IGF-1 in the bone matrix may not be sufficiently available for new bone formation during the aging process. Therefore, modulation of IGF-1 deposition in the bone matrix could potentially be a therapeutic approach to delay or prevent osteoporosis.

METHODS

Methods and any associated references are available in the online version of the paper.

Note: Supplementary information is available in the online version of the paper.

ACKNOWLEDGMENTS

The project described was supported by grant AR 053973 (X.C.) from NIAMS/NIH. J.C. is supported by grant T32DK007751v from the US National Institutes of Health. The authors thank B.J. Canning (Asthma and Allergy Center, Johns Hopkins University) for providing guinea pig marrow cells.

AUTHOR CONTRIBUTIONS

L.X., X.W., M.L. and L.P. performed the majority of the experiments, analyzed data and prepared the manuscript. T.Q. maintained mice, collected tissue samples and helped with micro-CT analyses. L.P. helped with the *in vitro* transwell migration assay. J.P.R. finished the human sample detection. X.J. and L.Z. assisted with rat *in vivo* experiments. J.C., F.F., C.J.R., S.Y., S.X., A.E. and M.W. provided suggestions for the project and critically reviewed the manuscript. X.C. supervised the project and wrote most of the manuscript.

COMPETING FINANCIAL INTERESTS

The authors declare no competing financial interests.

Published online at http://www.nature.com/doifinder/10.1038/nm.2793.
Reprints and permissions information is available online at http://www.nature.com/reprints/index.html.

1. Rizzoli, R., Bianchi, M.L., Garabedian, M., McKay, H.A. & Moreno, L.A. Maximizing bone mineral mass gain during growth for the prevention of fractures in the adolescents and the elderly. *Bone* **46**, 294–305 (2010).
2. Schettler, A.E. & Gustafson, E.M. Osteoporosis prevention starts in adolescence. *J. Am. Acad. Nurse Pract.* **16**, 274–282 (2004).
3. Teitelbaum, S.L. Bone resorption by osteoclasts. *Science* **289**, 1504–1508 (2000).
4. Zaidi, M. Skeletal remodeling in health and disease. *Nat. Med.* **13**, 791–801 (2007).
5. Agnusdei, D. & Gentilella, R. GH and IGF-I as therapeutic agents for osteoporosis. *J. Endocrinol. Invest.* **28**, 32–36 (2005).
6. Belfiore, A., Frasca, F., Pandini, G., Sciacca, L. & Vigneri, R. Insulin receptor isoforms and insulin receptor/insulin-like growth factor receptor hybrids in physiology and disease. *Endocr. Rev.* **30**, 586–623 (2009).
7. Giustina, A., Mazziotti, G. & Canalis, E. Growth hormone, insulin-like growth factors, and the skeleton. *Endocr. Rev.* **29**, 535–559 (2008).
8. Yakar, S. & Rosen, C.J. From mouse to man: redefining the role of insulin-like growth factor-I in the acquisition of bone mass. *Exp. Biol. Med. (Maywood)* **228**, 245–252 (2003).
9. Yakar, S., Pennisi, P., Wu, Y., Zhao, H. & LeRoith, D. Clinical relevance of systemic and local IGF-I. *Endocr. Dev.* **9**, 11–16 (2005).
10. Amin, S. *et al.* High serum IGFBP-2 is predictive of increased bone turnover in aging men and women. *J. Bone Miner. Res.* **22**, 799–807 (2007).
11. Ohlsson, C. *et al.* The role of liver-derived insulin-like growth factor-I. *Endocr. Rev.* **30**, 494–535 (2009).
12. Seck, T. *et al.* Concentration of insulin-like growth factor (IGF)-I and -II in iliac crest bone matrix from pre- and postmenopausal women: relationship to age, menopause, bone turnover, bone volume, and circulating IGFs. *J. Clin. Endocrinol. Metab.* **83**, 2331–2337 (1998).
13. Yamaguchi, T. *et al.* Serum levels of insulin-like growth factor (IGF); IGF-binding proteins-3, -4, and -5; and their relationships to bone mineral density and the risk of vertebral fractures in postmenopausal women. *Calcif. Tissue Int.* **78**, 18–24 (2006).
14. Hill, P.A. Bone remodelling. *Br. J. Orthod.* **25**, 101–107 (1998).
15. Abe, E. *et al.* TSH is a negative regulator of skeletal remodeling. *Cell* **115**, 151–162 (2003).
16. Mundy, G.R. & Elefteriou, F. Boning up on ephrin signaling. *Cell* **126**, 441–443 (2006).
17. Tang, Y. *et al.* TGF-β1–induced migration of bone mesenchymal stem cells couples bone resorption with formation. *Nat. Med.* **15**, 757–765 (2009).
18. Bautista, C.M., Mohan, S. & Baylink, D.J. Insulin-like growth factors I and II are present in the skeletal tissues of ten vertebrates. *Metabolism* **39**, 96–100 (1990).
19. Canalis, E., Pash, J., Gabbitas, B., Rydziel, S. & Varghese, S. Growth factors regulate the synthesis of insulin-like growth factor-I in bone cell cultures. *Endocrinology* **133**, 33–38 (1993).
20. Pfeilschifter, J. *et al.* Parathyroid hormone increases the concentration of insulin-like growth factor-I and transforming growth factor β 1 in rat bone. *J. Clin. Invest.* **96**, 767–774 (1995).
21. Hayden, J.M., Mohan, S. & Baylink, D.J. The insulin-like growth factor system and the coupling of formation to resorption. *Bone* **17**, 93S–98S (1995).
22. Rodda, S.J. & McMahon, A.P. Distinct roles for Hedgehog and canonical Wnt signaling in specification, differentiation and maintenance of osteoblast progenitors. *Development* **133**, 3231–3244 (2006).
23. Callewaert, F., Sinnesael, M., Gielen, E., Boonen, S. & Vanderschueren, D. Skeletal sexual dimorphism: relative contribution of sex steroids, GH-IGF1, and mechanical loading. *J. Endocrinol.* **207**, 127–134 (2010).
24. Russell, R.C., Fang, C. & Guan, K.L. An emerging role for TOR signaling in mammalian tissue and stem cell physiology. *Development* **138**, 3343–3356 (2011).
25. Harrison, D.E. *et al.* Rapamycin fed late in life extends lifespan in genetically heterogeneous mice. *Nature* **460**, 392–395 (2009).
26. Selman, C. *et al.* Ribosomal protein S6 kinase 1 signaling regulates mammalian life span. *Science* **326**, 140–144 (2009).
27. Liu, L. & Parent, C.A. Review series: TOR kinase complexes and cell migration. *J. Cell Biol.* **194**, 815–824 (2011).
28. Blüher, M., Kahn, B.B. & Kahn, C.R. Extended longevity in mice lacking the insulin receptor in adipose tissue. *Science* **299**, 572–574 (2003).
29. Bonjour, J.P., Chevalley, T., Ferrari, S. & Rizzoli, R. The importance and relevance of peak bone mass in the prevalence of osteoporosis. *Salud Publica Mex.* **51** (suppl. 1), S5–S17 (2009).
30. Liu, J.M. *et al.* IGF-1 as an early marker for low bone mass or osteoporosis in premenopausal and postmenopausal women. *J. Bone Miner. Metab.* **26**, 159–164 (2008).
31. Ohlsson, C. *et al.* Older men with low serum IGF-1 have an increased risk of incident fractures: the MrOS Sweden study. *J. Bone Miner. Res.* **26**, 865–872 (2011).
32. Hauschka, P.V., Mavrakos, A.E., Iafrati, M.D., Doleman, S.E. & Klagsbrun, M. Growth factors in bone matrix. Isolation of multiple types by affinity chromatography on heparin-Sepharose. *J. Biol. Chem.* **261**, 12665–12674 (1986).
33. Lamberts, S.W., van den Beld, A.W. & van der Lely, A.J. The endocrinology of aging. *Science* **278**, 419–424 (1997).
34. Tatar, M., Bartke, A. & Antebi, A. The endocrine regulation of aging by insulin-like signals. *Science* **299**, 1346–1351 (2003).
35. Ziv, E. & Hu, D. Genetic variation in insulin/IGF-1 signaling pathways and longevity. *Ageing Res. Rev.* **10**, 201–204 (2011).
36. Mohan, S. & Baylink, D.J. Serum insulin-like growth factor binding protein (IGFBP)-4 and IGFBP-5 levels in aging and age-associated diseases. *Endocrine* **7**, 87–91 (1997).
37. Boonen, S. *et al.* Musculoskeletal effects of the recombinant human IGF-I/IGF binding protein-3 complex in osteoporotic patients with proximal femoral fracture: a double-blind, placebo-controlled pilot study. *J. Clin. Endocrinol. Metab.* **87**, 1593–1599 (2002).

ONLINE METHODS

Mice and rats. We obtained *Rag*$^{-/-}$ mice from the Mouse Models of Human Cancers Consortium Repository, US National Cancer Institute. The *Igf1r*$^{flox/flox}$ and Osx1-GFP::Cre (The Jackson Laboratory) mouse lines have been described previously[22]. To generate Osx-Cre; *Igf1r*$^{flox/flox}$ (*Igf1r*$^{-/-}$) mice, we crossed hemizygous Osx-Cre transgenic mice with *Igf1r*$^{flox/flox}$ mice to generate heterozygous *Igf1r*^{flox} offspring with or without a Cre allele. We then intercrossed these offspring to generate the following offspring: Osx-Cre; *Igf1r*$^{flox/flox}$ (conditional knockout mice referred as *Igf1r*$^{-/-}$), Osx-Cre (referred as *Igf1r*$^{+/+}$), Osx-Cre; *Igf1r*$^{flox/+}$ (heterozygous conditional knockout mice, referred to as *Igf1r*$^{+/-}$) and mice without Osx-Cre. The LID mice were created by crossing the mice expressing Cre recombinase under the albumin enhancer and promoter (The Jackson Laboratory) with the mice floxed at exon 4 of the *Igf1* gene[38]. We performed genotyping using the genomic DNA isolated from tail biopsies. We purchased different aged male Sprague Dawley rats from Harlan Laboratories and used 20-month-old male rats (referred to here as old rats) in the local injection experiment. The average body weight of the old rats was 675 ± 25 g (mean ± s.e.m.). All animals were maintained in the Animal Facility of the Johns Hopkins University School of Medicine. The experimental protocol was reviewed and approved by the Institutional Animal Care and Use Committee of Johns Hopkins University, Baltimore, MD, USA.

Isolation and culture of mouse MSCs. We collected bone marrow cells from 6-week-old male *Igf1r*$^{flox/flox}$ and wild-type mice euthanized by cervical dislocation and cultured cells with minimum essential medium α (α-MEM, Mediatech, Inc.) supplemented with penicillin (100 U ml^{-1}, Sigma-Aldrich), streptomycin sulfate (100 μg ml^{-1}, Sigma-Aldrich) and 20% lot-selected FBS (FBS, Atlanta Biologicals) at 37 °C in a 5% CO_2 humidified incubator. After 72 h of adhesion, we removed nonadherent cells and cultured adherent cells for an additional 7 d with a single media change. The adherent cells were then retrieved by trypsin digestion. We incubated the cell aliquots for 20 min at 4 °C with phycoerythrin (PE)-, FITC-, peridinin chlorophyll protein (Per CP)- and allophycocyanin (APC)-conjugated antibodies to mouse Sca-1, CD29, CD45 and CD11b (BioLegend) (see the antibody list in the **Supplementary Methods** for further information about the antibodies used). Acquisition was performed on a fluorescence-activated cell sorting (FACS) Aria model (BD Biosciences), and the analysis was performed using FACS DIVE software version 6.1.3 (BD Biosciences). The sorted CD29^{+}Sca-1^{+}CD45^{-}CD11b^{-} cells were enriched by further culture.

Adenoviral infection. For the adenoviral infections, we plated MSCs at a density of 5 × 10^5 cells in 100-mm plates. We added Ad-Cre-GFP viruses to the MSCs at a multiplicity of infection of 100 and suspended them in PBS at 37 °C in a 5% CO_2 atmosphere. Plates were swirled every 15 min, and fresh α-MEM with 10% FBS was added after 1 h of incubation. We exposed the cells to fresh α-MEM containing adenovirus for 48 h. The control group (Ad-GFP instead of Ad-Cre-GFP) was treated following the same method. We obtained the adenovirus preparations from Vector Biolabs (Philadelphia, PA).

RNA interference. We transfected MSCs with siRNA targeting *Irs1* or scrambled control siRNA that has been tested to not lead to the specific degradation of any known cellular mRNA (Santa Cruz) using Lipofectamine RNAiMAX in Opti-MEM (Invitrogen) according to the protocol recommended by the manufacturer (Invitrogen). Experiments were performed 48 h after transfection. Neither the scrambled siRNA nor the siRNA targeting *Irs1* had a marked effect on cellular morphology. We validated the successful knockdown of IRS1 using a western blot analysis.

CFU-F and CFU-Ob assays. At the time of euthanasia, we collected bone marrow from femoral, tibial and humeral medullary cavities of the mice and determined the cell numbers with Zap-OGLOBIN (Coulter Corp.) after removal of the red blood cells. The numbers of CFU-Fs and CFU-Obs in mouse bone marrow isolates and cocultures with irradiated guinea pig marrow cells were as reported[39]. We obtained marrow cells from the femora and tibiae of 2-month-old female Hartley guinea pigs by flushing with a 22-gauge needle and then resuspended the cells. We gamma irradiated cells with a cobalt-57 source for 50 min at 1.2 Grays min^{-1}, as reported[40]. After rinsing by centrifugation, cells were resuspended in α-MEM medium with 20% FBS, counted and cultured at 2.5 × 10^6 cells per well of a six-well plate. For the assay of the number of CFU-Fs and CFU-Obs, we plated 0.1 × 10^5, 0.5 × 10^5 or 1 × 10^5 mouse marrow cells into six-well plates in 3 ml α-MEM supplemented with glutamine (2 mM), penicillin (100 U ml^{-1}), streptomycin sulfate (100 μg ml^{-1}) and 20% lot-selected FBS. We also established duplicate cultures. After 2–3 h of adhesion, we removed unattached cells and added 2.5 × 10^6 irradiated guinea pig feeder cells (provided by B.J. Canning) to the cultivation medium of the adherent cultures just after washing. On day 14, we fixed and stained the cultures with 0.5% crystal violet. We counted the colonies that contained 50 or more cells. For the CFU-Ob assay, we cultured the cells with osteogenic medium (10% FBS, 10^7 M dexamethasone, 10 mM β-glycerol phosphate and 50 μM ascorbate-2-phosphate) for 21 d and analyzed them with Alizarin red staining. We determined the colony-forming efficiency by quantifying the number of colonies per 10^5 marrow cells plated.

Bone marrow cavity transplantation. We used 3-month-old male *Rag2*$^{-/-}$ mice with an immune-deficient background as recipients. We injected GFP-labeled cells in 10 μl of α-MEM media into the bone marrow cavity of the left femora of the mice, as previously described. The mice were euthanized 2 or 4 weeks after transplantation, and the distal femora were processed for staining. In some cases, we collected cells from the bone marrow and compact bones by collagenase digestion and assessed the total number of GFP^{+} cells by a flow cytometry analysis. Bone surface GFP^{+} cells were calculated as cells per millimeter of perimeter in sections, and bone matrix GFP^{+} cells were calculated as cells per mm^2 of matrix area in sections.

Subrenal capsule transplant. We used 2-month-old male *Rag2*$^{-/-}$ mice with an immune-deficient background as recipients. We inoculated 5 × 10^3 GFP-labeled cells in Matrigel (with 100 ng ml^{-1} IGF-1) underneath the renal capsule of mice injected subcutaneously with rapamycin (3 mg per kg body weight per day) or vehicle 1 day before transplant and then daily for 4 weeks. We euthanized the mice 4 weeks after transplantation and processed the kidneys for frozen histology staining.

***In vitro* osteoblastic differentiation.** We plated MSCs cells at a density of 1,000 cells per well in the six-well plates and expanded them in growth medium for 3 d. We induced osteoblastic differentiation in low serum conditions (2% FBS) in differentiation medium (α-MEM supplemented with 50 μg ml^{-1} ascorbic acid and 10 mM β-glycerol phosphate). We added 100 ng ml^{-1} mouse recombinant IGF-1 (Abcam) to the differentiation medium with or without the PI3K inhibitor LY294002 (10 μM) or the mTOR inhibitor rapamycin (20 nM). We changed the medium every 3 d and assayed the cellular differentiation 20 d after induction using Alizarin red staining.

Micro-CT analysis. We obtained long bone from mice and rats, dissected it free of soft tissue, fixed it overnight in 70% ethanol (for mice) or 10% formalin (for rats) and analyzed it using high-resolution micro-CT (SkyScan1076 *in vivo* CT for mice, SkyScan1172 *in vivo* CT for rats). We used image reconstruction software (NRecon v1.6), data analysis software (CTAn v1.9) and three-dimensional model visualization software (μCTVol v2.0) to analyze the parameters of the trabecular bone in the metaphysis. We set the scanner at a voltage of 89 kVp for mice or 50 kVp for rats, a current of 112 μA for mice or 200 μA for rats and a resolution of 8.66596 μm pixel^{-1} for mice or 12.1 μm pixel^{-1} for rats. We established cross-sectional images of the proximal tibiae and femora to perform a three-dimensional histomorphometric analysis of the trabecular bone. The sample area selected for scanning was a 1.5-mm length of the metaphyseal secondary spongiosa, originating 1.0 mm below the epiphyseal growth plate and extending caudally. For the aged rats, we used cross-sectional images of the distal femur to perform three-dimensional and two-dimensional morphometric analyses of the trabecular bone (400 cross sections per specimen).

Histochemistry, immunohistochemistry and histomorphometric analyses. At the time of euthanasia, we dissected the tibiae or femora of the mice and fixed the specimens in 10% buffered formalin for 48 h, decalcified them in 10% EDTA (pH 7.0) for 14 d and embedded them in paraffin. Longitudinally

doi:10.1038/nm.2793

oriented 4-μm–thick sections of bone including the metaphysis and diaphysis were processed for TRAP staining (Sigma-Aldrich) and Goldner's trichrome staining. For immunohistochemical staining, we incubated the sections with primary antibodies overnight at 4 °C and used a horseradish peroxidase–streptavidin detection system (Dako) to detect immunoreactivity, which was followed by counterstaining with hematoxylin (Dako) or methyl green (Sigma-Aldrich). We used isotype-matched negative control antibodies (antibodies that were not to the specific proteins to be detected) (R&D Systems) under the same conditions. We performed histomorphometric measurements of the two-dimensional parameters of the trabecular bone in the secondary spongiosa in a 2-mm square, 1 mm distal to the lowest point of growth plate, with OsteoMeasureXP Software (OsteoMetrics, Inc.). To label the mineralization fronts, the mice were given subcutaneous injections of calcein (Sigma, 15 mg per kg body weight) in 2% sodium bicarbonate solution 10 d and 3 d before death. We selected all histomorphometric parameters in four random visual fields per specimen and measured five specimens per mouse in each group.

Western blot analysis and ELISA. We prepared the MSCs cell lysates from adenovirus infection, siRNA-transfected and inhibitor-treated assays in 2% sodium dodecyl sulfate, 2 M urea, 10% glycerol, 10 Mm Tris-HCl (pH 6.8), 10 mM dithiothreitol and 1 mM phenylmethylsulfonyl fluoride. We performed western blot analyses in conditional media or on the protein of lysates from the individual groups. We centrifuged the lysates and separated the supernatants by SDS-PAGE, blotted them onto a polyvinylidene fluoride (PVDF) membrane (Bio-Rad Laboratories), analyzed them with specific antibodies and visualized them by enhanced chemiluminescence (ECL Kit, Amersham Biosciences). We used antibodies recognizing mouse IGF-1 (R&D Systems, Inc., 1:1,000), IGF1R (Cell Signaling technology Inc.1:1,000) and β-actin (Sigma-Aldrich. AC-74, 1:10,000) to examine the concentrations of IGF-1 in conditional media and the concentrations of IGF1R protein in the lysates. We detected the amount of IGF-1 in the conditioned media with a DuoSet ELISA Development Kit (R&D Systems, DY 791) according to the manufacturer's instructions. Antibodies to IRS1, PI3K, Akt and mTOR are listed in the **Supplementary Methods**. The phosphorylation IRS-1 was detected with an anti-phosphotyrosine antibody (4G10, Upstate) after immunoprecipitation with the specific antibodies.

***In vitro* bone resorption assays.** For the preparation of osteoclastic BRCM, we isolated bone marrow macrophages from the long bones of mice and cultured them in α-MEM containing 10% heat-inactivated FBS in the presence of macrophage colony-stimulating factor (M-CSF). We cultured the cells for 2 d in the presence of 10 ng ml^{-1} recombinant M-CSF (R&D Systems Inc.) and then plated the cells onto bone slices of bovine cortical bone in 24-well tissue culture plates (1×10^5 cells per well) and in the presence of 10 ng ml^{-1} recombinant M-CSF and 100 ng ml^{-1} receptor activator of nuclear factor κB ligand (RANKL). Under these conditions, osteoclasts began to form and resorb bone after 6 to 7 d. The cultured cells were stained for TRAP activity after 8–10 d using a commercial kit (Sigma-Aldrich). We determined the resorption of the bovine cortical bone slices by scanning electronic microscopy. We harvested the conditioned media from the osteoclast-mediated resorption after 8–10 days by centrifugation. We added neutralizing antibodies to IGF-1 (R&D System, Inc., 2 μg ml^{-1}), IGF-II (R&D System, Inc., 1 μg ml^{-1}) and PDGF (R&D System, Inc., 5 μg ml^{-1}), to the conditioned media. Noggin (BD Biosciences) was added to a final concentration of 100 ng ml^{-1}.

Bone marrow cavity injection of IGF-1, IGFBP3 and IGF-1 with IGFBP3. We randomly divided 40 rats into four groups with ten rats per group. We purchased recombinant IGF-1 and IGFBP3 from Abcam and R&D Systems. We delivered IGF-1 (8 μg), IGFBP3 (42 μg), IGF-1 with IGFBP3 (8 μg of IGF-1 and 42 μg of IGFBP3 at a molar ratio of 1:1) or vehicle (PBS) into the bone marrow cavity of the mice once a week, injected from the medial side of the patellar tendon using 0.5 ml-syringes with 27-gauge needles. We collected whole blood samples by cardiac puncture for biochemical assessments immediately after euthanasia by CO_2 asphyxiation after 4 weeks. We collected blood samples by centrifugation to obtain the sera, which we then stored at −80 °C until assayed.

Bone matrix extraction and bone marrow serum collection. We exposed bone marrow from freshly euthanized rats at the growth plate and placed the samples for centrifugation with the trabecular part of the bone at the top. We removed the bone marrow by centrifugation of the samples for 15 min at 5,000 rpm and 4 °C. We immersed the resected femora in liquid nitrogen and mechanically crushed the specimens into small fragments of several millimeters in diameter. The fragments were washed repeatedly in cold distilled water until they were free of blood and were then defatted in cold isopropyl ether. We grounded the defatted bone fragments into smaller particles using a biopulverizer (BioSpec Products, Inc., Bartlesville, OK, USA). We placed 40–50 mg of the particles in a mini dialysis unit with a 3.5 kDa molecular weight cutoff (Termo). We added 0.5 ml of extraction solution (4 M guanidine-HCl, 0.05 M EDTA, 30 mM Tris and 1 mg ml^{-1} BSA, pH 7.4) with protease inhibitors (1 mM phenylmethyl–sulfonyl fluoride, 5 mM benzamidine-HCl, 0.1 M E–aminocaproic acid and 2 μg ml^{-1} leupeptin) into the mini dialysis unit to decalcify the bone tissue and to extract proteins from the bone matrix. The mini dialysis tube was in contact with the extraction solution in a beaker (500 ml for 15 mini dialysis units). We conducted the extraction procedure at 4 °C on a stir plate with a low-speed setting for 48 h. We then re-dialyzed the bone sample against a PBS solution for 72 h at 4 °C. Finally, we stored the extracts at −80 °C until assaying them for growth factor activity.

Systemic infusion by osmotic pumps. IGF-1 (1.5 mg per kg body weight per day), IGF-1 plus IGFBP3 (1.5 mg per kg body weight per day IGF-1 and 7.8 mg per kg body weight per day IGFBP3 at a molar ratio of 1:1) or vehicle was infused into the circulation of 4-week-old female LID mice with osmotic pumps for 4 weeks. Osmotic pumps (ALZET) were embedded subcutaneously.

Measurement of IGF-1 and IGFBP3 concentrations. We determined the concentration of IGF-1 using either a mouse or rat IGF-1 Immunoassay Kit (ELISA) (R&D Systems) according to the instructions provided. This assay was designed to eliminate interference by binding proteins. We diluted the peripheral blood serum 1,000-fold, the bone marrow serum 500-fold and the bone matrix protein tenfold with the Calibrator Diluent RD5-38 before detection. The assay sensitivity was 3.5 pg ml^{-1}; the intra-assay and interassay coefficients of variation were 5.6% and 4.3%, respectively. We assessed human IGF-1 concentration (from the samples described in the next section) by ELISA after an acid-ethanol extraction. The interassay variation was 5.3%, and the intra-assay variation was 2.3%. We determined the concentration of IGFBP3 using either a mouse or rat IGFBP3 Immunoassay Kit (ELISA) (BioVendor) according to the instructions provided. The assay sensitivity was 18 pg ml^{-1}; the intra-assay and interassay coefficients of variation were 4.6% and 8.4%, respectively.

Collection of human bone marrow samples. We collected bone marrow samples from individuals with osteoporosis, as defined by hip fractures and low bone mass ($n = 12$), and individuals of similar ages with osteoarthritis and normal bone mineral density ($n = 12$). The bone marrow collection was performed during total hip replacement with informed consent and approval by the Institutional Review Board at the University of Chile. Detailed information on the samples is given in **Supplementary Table 2**.

Statistics. Data are presented as the mean ± s.e.m. and were analyzed using one-way ANOVA followed by Dunnett's test, two-tailed *t* test or Bonferroni test.

38. Yakar, S. *et al.* Normal growth and development in the absence of hepatic insulin-like growth factor I. *Proc. Natl. Acad. Sci. USA* **96**, 7324–7329 (1999).
39. Kuznetsov, S. & Gehron, R.P. Species differences in growth requirements for bone marrow stromal fibroblast colony formation *in vitro*. *Calcif. Tissue Int.* **59**, 265–270 (1996).
40. Di Gregorio, G.B. *et al.* Attenuation of the self-renewal of transit-amplifying osteoblast progenitors in the murine bone marrow by 17 β-estradiol. *J. Clin. Invest.* **107**, 803–812 (2001).